COMBUSTION AND FLAME 36:245–262 (1979)

A Mathematical Model of Evaporation–Pyrolysis Processes Inside a Naturally Smoldering Cigarette

MOTOHIKO MURAMATSU, SETSUKO UMEMURA, and TAKASHI OKADA

Central Research Institute, The Japan Tobacco and Salt Public Corporation, 6-2 Umegaoka, Midori-ku, Yokohama, Kanagawa 227, Japan

A one-dimensional mathematical model for heat and mass balance has been proposed to elucidate the changes occurring in the temperature and density of the evaporation-pyrolysis zone in a naturally smoldering cigarette. The model considers: (1) pyrolysis of tobacco obeying Arrhenius kinetics, (2) evaporation of water from tobacco following a mass-transfer- and rate-determined process, (3) weight loss of tobacco due to pyrolysis and evaporation, (4) internal heat transfer characterized by effective thermal conductivity, (5) heat loss attributable to free convection and radiation from the outer surface of the cigarette and endothermicity of the evaporation process, and (6) smoldering speed. These processes are expressed in a set of simultaneous ordinary differential equations that can be solved numerically by the Runge-Kutta-Gill method.

The calculated distribution profiles of temperature and density in the evaporation-pyrolysis zone approximate the experimental results measured using thermocouples and a β-ray attenuation technique. On the basis of the model, the influences of several physical parameters on the shapes of the temperature and density profiles are predicted.

INTRODUCTION

The temperature distribution inside a smoldering cigarette plays an important role in the formation of smoke [1]. This temperature distribution has been studied extensively [1-6], but the physicochemical factors governing smoldering speed and temperature and the fundamental mechanism of smoldering are not well documented.

Egerton et al. [7] and Gugan [8] have studied the smoldering of cigarettes under conditions of intermittent puffing and/or natural convection. Jenkins et al. [9] have measured the changes in the density of a smoldering cigarette and correlated them with the temperature distribution reported by Baker [6]. Based on experimentally determined temperature and gas distributions, Baker [10] has recently estimated, using simplified heat- and mass-transfer equation, the rate of chemical production of heat and carbon oxides inside a steadily smoldering cigarette. A theoretical and experimental investigation of the smoldering mechanism of a cylindrical cellulosic material, not tobacco, has been conducted by Moussa et al. [11]. Their model excellently accounts for the effects of oxygen mole fraction and partial pressure on smoldering speed, temperature, and extinguishment limit.

According to the above works, two major reaction zones exist in a smoldering cigarette: (1) the high-temperature burning zone (above 500°C) and (2) the evaporation-pyrolysis zone (100–500°C). Moreover, many factors, such as reaction rate and mass and heat transfer influence the processes occurring in the two smoldering zones. Since the available experimental data and theoretical interpretations do not completely define the mechanism of smoldering, we have been investigating the natural smoldering of cigarettes by: (1) surveying the effective thermal conductivity in cigarette columns and the specific heat of tobacco [12], (2) conducting thermal analyses of tobacco and its

0010-2180/79/090245+18$01.75

TABLE 1

Properties of Test Cigarettes

Cigarette (symbol)	Tobacco type	Weight (g/cig)	Pressure drop (mm H_2O)	Packing density (g/cm^3)	Water content (wt. %)[a]	Apparent density of shred (g/cm^3)	Real density of shred (g/cm^3)
F	Flue cured	0.99	48	0.281	13.11	0.824	1.392
B	Burley	0.90	82	0.256	10.90	0.736	1.440
M_1	Matsukawa	0.74	46	0.210	11.34	0.691	1.386
M_2	Matsukawa	0.84	68	0.239	11.34	0.691	1.386
M_3	Matsukawa	1.03	137	0.293	11.34	0.691	1.386

[a] Dry base.

carbonaceous residue, (3) estimating oxygen consumption and heat evolution during smoldering [13], (4) developing a realistic theoretical model of the evaporation-pyrolysis zone that can predict the changes in temperature and density inside a naturally smoldering cigarette at a given smoldering speed and specified physical parameters, (5) establishing an overall theory of natural smolder, considering both the burning zone and the evaporation-pyrolysis zone, from which smoldering speed and temperature distribution can be predicted.

In the present paper we have developed a model of the evaporation-pyrolysis zone using the experimental results of our survey of cigarette thermal properties and our thermal analyses of tobacco. On the basis of the postulated mechanism of natural smoldering, a one-dimensional heat and mass-balance model expressed by a set of simultaneous ordinary differential equations is presented. The distribution profiles of both temperature and density obtained from the numerical solutions of those equations agree well with the experimentally determined curves.

EXPERIMENTAL METHODS

Samples

Several nonblended cigarettes 70 mm long and 8 mm in diameter were tested (Table 1). The cigarettes were selected for weight and pressure drop at an airflow of 17.5 cm^3/sec after conditioning at 20°C and 60% relative humidity.

Measurements of Temperature and Smoldering Speed

A pair of thermocouples was used to measure the smoldering temperature and the smoldering rate of the test cigarettes. The thermocouples [Pt-Pt (87%)·Rh (13%), 0.05 mm diameter] were inserted across the cigarette with their junctions positioned on the central axis; one was 20 mm and the other 40 mm from the lit end. The ends of the thermocouple wires were led to a two-pen recorder, and temperature-time curves were recorded at both positions during the natural smoldering. Since the two temperature-time curves could be almost superposed (i.e., the natural smoldering could be regarded as stationary as described in an earlier paper [4]), the smoldering speed was determined from the time lag between the two temperature-time curves and the distance between the two thermocouples.

One-dimensional distribution curves of temperature along the longitudinal axis of the cigarette were generated from the temperature-time curves and the smoldering speed.

Measurements of Density

Changes in the density and temperature of a naturally smoldering cigarette were measured simultaneously to clarify the relationship between these variables. The measurements of the changes in density were made by a β-ray attenuation technique reported by Jenkins et al. [9] with some modifications.

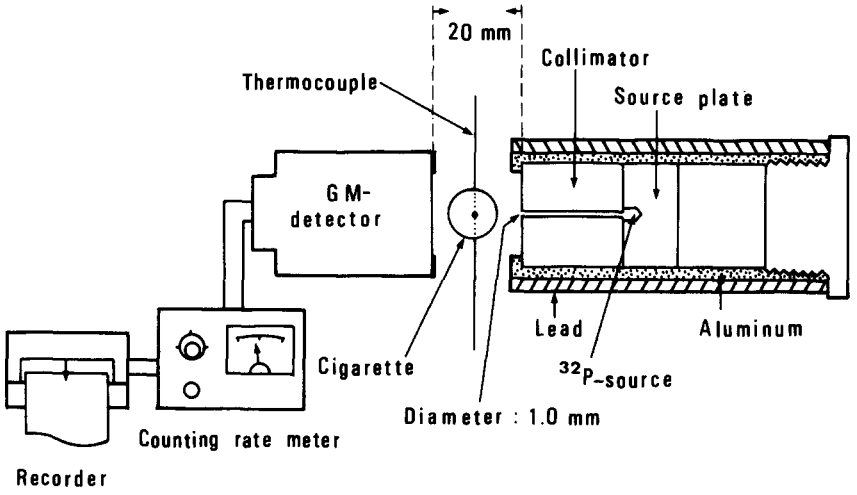

Fig. 1. Schematic diagram of apparatus for measuring change in density of a naturally smoldering cigarette.

A diagram of the measuring system is schematically shown in Fig. 1. A solution of orthophosporic acid containing 2 mCi of ^{32}P (Japan Radio Isotope Assoc.) was diluted with 10^{-3}-M sodium biphosphate until the total volume of the solution was about 100 μl. The ^{32}P-containing solution was then transferred into an aluminum cell (ϕ3 mm X 5 mm) mounted in a cylindrical source plate (ϕ30 mm X 15 mm) made of polyvinyl chloride. After removal of water, the residual ^{32}P was covered with a thin film of collodion. A cylindrical collimator (ϕ30 mm X 30 mm) made of lead and having a slit hole 1.0 mm in diameter along its central axis was also used. The source plate and collimator were put in series in a double-walled cylinder, with a 3-mm-thick wall of aluminum and a 6-mm-thick outside wall of lead.

The intensity of the β-ray beam coming from the collimator was measured with a Geiger-Müller (GM) detector (Aloka Co., Ltd., Model GM-2503A, 1100 V) connected to a counting rate meter (Aloka Co., Ltd., Model PRM-401B) and then to a recorder. The GM detector and the source cylinder were positioned so that the collimator slit was perpendicular to the window of the detector. A cigarette fitted with a pair of thermocouples was held in the space between the window and the collimator and positioned so that the β-ray beam intercepted it perpendicular to its central axis at a point 20 mm from the lit end. The change in the intensity of the β-ray beam was then measured as the cigarette smoldered.

Recorded counting rate-time curves, as well as temperature-time curves, were transformed into digital data and punched onto paper tape for the computer at 2-sec intervals using a curve reader (Auto Process Corp., Model 5801). The β-ray count was corrected for dead time of the detector, insertion of the thermocouple, and background on all measurements. The counting rate-time curves were smoothed by the method of Savitzky and Golay [14] to minimize scatter caused by the random decay of ^{32}P. The smoothed curves were converted into density-time curves using a density-counting-rate calibration curve and then into the axial distribution curves for density in a manner similar to that used to generate temperature-distribution curves.

The density-counting-rate calibration curve was developed using a series of unlit cigarettes and cigarette filters (8 mm in diameter) with widely different densities (0.06-0.36 g/cm^3). The following empirical equation describes the calibration curve:

$$\log \frac{I}{I_0} = -2.128\rho.$$

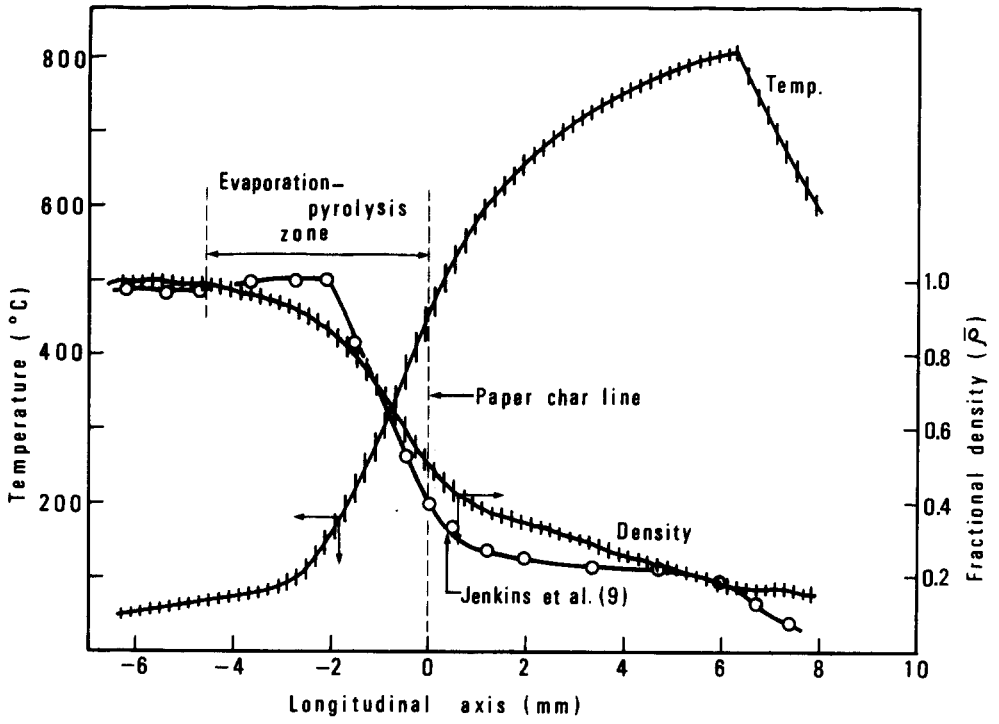

Fig. 2. Typical temperature and density profiles and their scatter.

The cigarette changes in chemical composition from virgin tobacco to ash during smoldering. However, the calibration constant does not change appreciably during this chemical transformation because the absorption of various ionizing radiations is directly related to the mass per unit area of the absorbing material and is independent of the nature of the material [15]. This was experimentally confirmed by comparing the β-ray absorption of a tablet of virgin tobacco with that of a tablet of ash as a function of the mass per unit area of the tablets.

All experiments were repeated at least six times, and the average was reported as the experimental value.

EXPERIMENTAL RESULTS

Figure 2 shows typical temperature and density profiles for cigarettes containing flue-cured tobacco. The figure also indicates the degree of data scatter in terms of the 95% confidence limit of each mean point. In this study the paper char line is considered to be at an axial position of zero, and positions on the unburned tobacco rod are given as negative distances from the paper char line. The degree of scatter of the temperature and density profiles for the other types of cigarette tested in this study (Table 1) is similar to that indicated in Fig. 2 for the cigarettes containing flue-cured tobacco.

Figure 3 shows temperature and density profiles for three typical cigarettes containing different tobacco types and Fig. 4, for cigarettes of one tobacco type but of different packing densities. These diagrams illustrate that the differences in temperature profiles of cigarettes of different tobacco types and packing densities are not statistically significant. However, density profiles differ somewhat for cigarettes of different tobacco con-

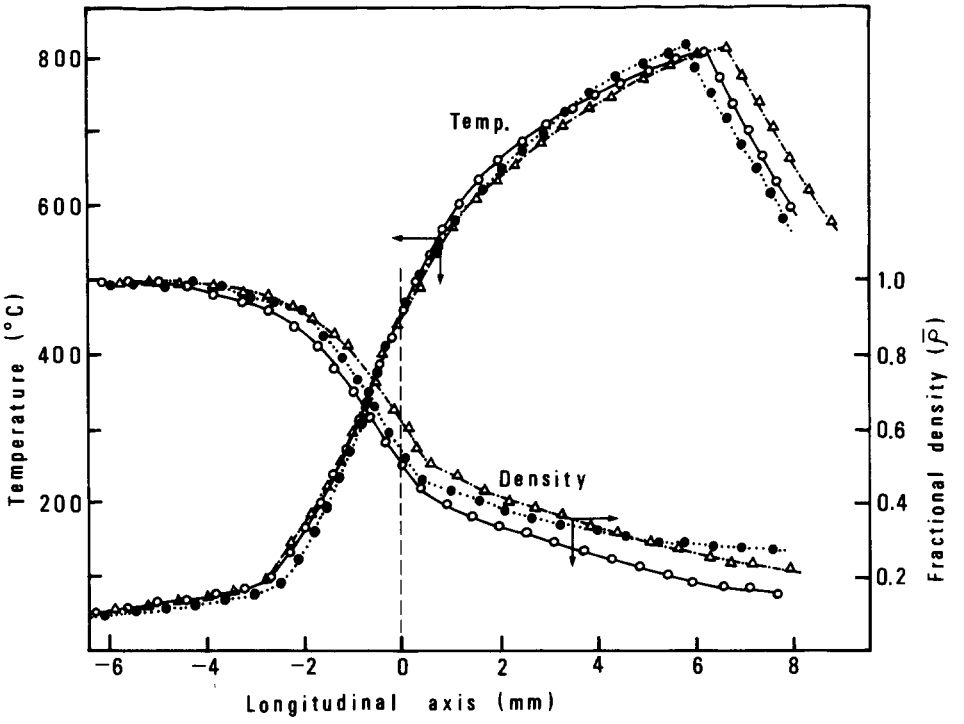

Fig. 3. Experimental temperature and density profiles for cigarettes containing different types of tobacco: –o—o–, flue cured (F); ··●·····●··; burley (B); –Δ–·–Δ–; Matsukawa (M_2).

tent. A discernible decrease in density, probably attributable to the evaporation of water in the tobacco, begins at 60-70°C, 4-5 mm from the paper char line. A relatively rapid decrease, which is most likely due to the pyrolysis of tobacco constituents accompanied by the formation of many smoke components and residual char, then occurs in the temperature range of about 200-500°C. Finally, this rapid decline is followed by a gradual decrease corresponding to char oxidation in the burning coal.

In all of the test cigarettes, the paper char line appeared when the temperature reached about 450°C. Since the char line can be considered to be a boundary line between the evaporation-pyrolysis zone and the burning zone, the thickness of the evaporation-pyrolysis zone seems to be about 4-5 mm.

Figure 2 also presents the density profile reported by Jenkins et al. [9] for a naturally smoldering cigarette. The decrease in density found in the present work started at a lower temperature and was more moderate than that measured by Jenkins et al. The temperature profiles determined in the present study agree well with those observed by earlier workers [2, 3].

FORMULATION OF A ONE-DIMENSIONAL MODEL

Data presented previously have demonstrated that the smoldering of cigarettes under the condition of natural convection is kept at a steady state [4] and that the radial distribution of the temperature within the cigarette is relatively flat at the evaporation-pyrolysis zone behind the burning coal [4, 6].

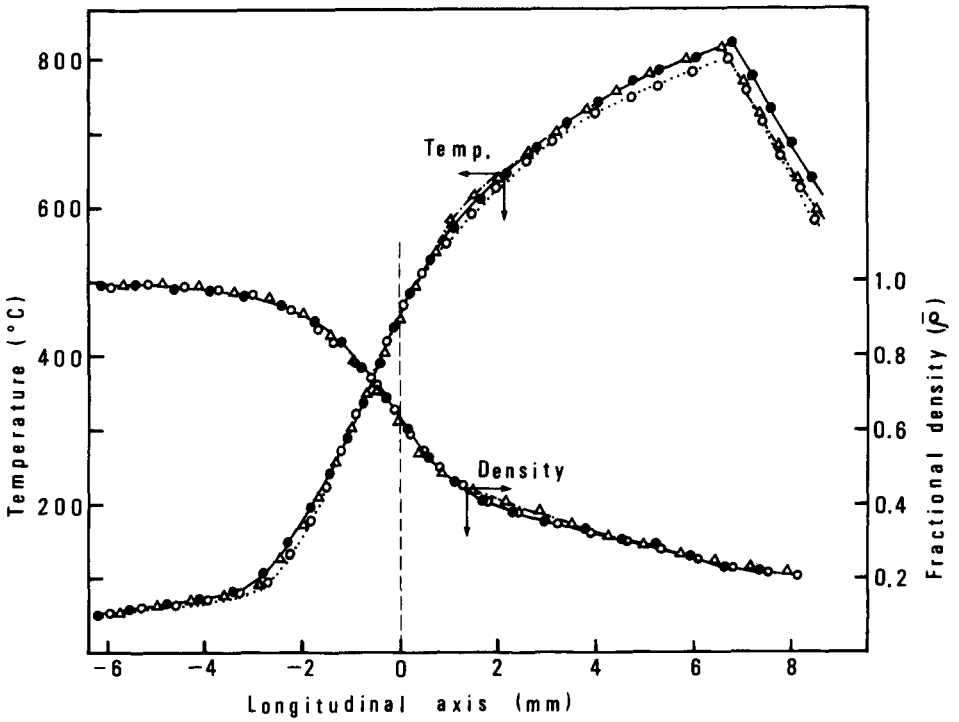

Fig. 4. Experimental temperature and density profiles for cigarretts with different packing densities: ··o·····o··; Matsukawa (M_1) (packing density = 0.210); –Δ–·–Δ–; Matsukawa (M_2) (packing density = 0.239); –•—•–; Matsukawa (M_3) (packing density = 0.293.

Therefore, a one-dimensional stationary model involving heat and mass balance can be formulated as follows.

The z-coordinate is taken along the longitudinal axis of the cigarette in the direction opposite to the advancing direction of smoldering. Since any analysis of the smoldering mechanism should be realistic and relatively simple, the following assumptions have been made to formulate heat and mass balance at a given small element of thickness dz between z and $z + dz$:

1. As the temperature of the element is raised by the heat flow transferred from the burning coal, virgin tobacco is continuously converted into volatile smoke components and residual char and water in the tobacco is evaporated.

Virgin tobacco — (pyrolysis) → Volatile smoke + residual char.

Water in tobacco — (evaporation) → Water vapor.

The smoke and water vapor leave the element through the outer surface of the cigarette. Consequently, the partially pyrolized element consists of unpyrolyzed virgin tobacco, residual char, and unevaporated water.

2. No smoke or water vapor recondenses in the element.
3. Atmospheric oxygen does not react with the virgin tobacco, char, or smoke in the element. This assumption has been made because of the interior of the pyrolysis zone has been reported to be oxygen deficient [1, 16].
4. The solid phase and the gas phase inside the element are at the same temperature. According to the temperature distribution reported by Baker [6], this assumption seems to be reasonable in the case of natural smoldering.
5. Heat loss from the outer surface of the

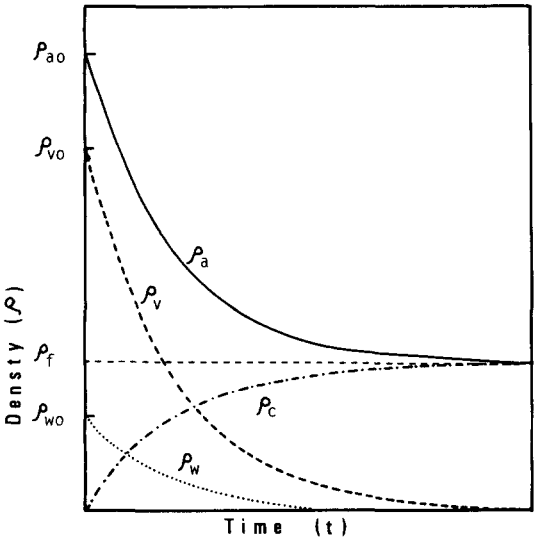

Fig. 5. An idealized model of changes in density at a given temperature. Density, ρ, is defined as the weight of each material per unit volume of a cigarette. The subscripts are defined as: v, virgin tobacco; c, char; w, water; 0, initial value; f, final value; a, total value.

element is caused by free convection and radiation.

6. Gas flow inside the cigarette column along the longitudinal axis is negligible during natural smoldering.
7. Heat flowing out of the element with the evolved smoke and water vapor is negligible compared with heat lost by free convection and radiation.
8. Heat transfer inside the cigarette column is caused by thermal conduction characterized by effective thermal conductivity.

Mass Balance

Figure 5 shows a model for changes in the density of virgin tobacco, water, and char in the element at a given temperature, T. As pyrolysis and evaporation proceed, the virgin tobacco and the water in that tobacco are gradually consumed (with the formation of residual char, smoke, and water vapor) and finally disappear, leaving only char with a final density, ρ_f. Here, let ρ be density and the subscripts, v, c, and w stand for virgin tobacco, char, and water, respectively. The total density, ρ_a, of the element at a given time is given by

$$\rho_a = \rho_v + \rho_c + \rho_w. \tag{1}$$

In this process the conversion of virgin tobacco into char and evolved smoke can be represented by

$$C = \frac{\rho_{v0} - \rho_v}{\rho_{v0}}. \tag{2}$$

Assuming that the reaction rate of the pyrolysis follows nth-order Arrhenius kinetics, the rate of the conversion is

$$\frac{\partial C}{\partial t} = -A \exp\left(-\frac{E}{RT}\right)(1 - C)^n. \tag{3}$$

The rate of decrease in the density of virgin tobacco is written by combining Eqs. 2 and 3 as follows:

$$\frac{\partial \rho_v}{\partial t} = -A \exp\left(-\frac{E}{RT}\right)\left(\frac{\rho_v}{\rho_{v0}}\right)^n \rho_{v0}. \tag{4}$$

As is described later, the actual reaction rate of pyrolysis of tobacco can be expressed as the summation of reaction rates for four major compounds; therefore, Eq. 4 can be rewritten as follows:

$$\frac{\partial \rho_v}{\partial t} = \sum_{i=1}^{4}\left(\frac{\partial \rho_{vi}}{\partial t}\right) = \sum_{i=1}^{4}\left\{-A_i \exp\left(-\frac{E_i}{RT}\right) \times \left(\frac{\rho_{vi}}{\rho_{v0i}}\right)^{n_i} \rho_{v0i}\right\}. \tag{5}$$

If the conversion of virgin tobacco into char is defined by ρ_f/ρ_{v0}, the rate of the increase in the density of the char is given by

$$\frac{\partial \rho_c}{\partial t} = -\frac{\rho_f}{\rho_{v0}}\frac{\partial \rho_v}{\partial t}. \tag{6}$$

On the other hand, the mechanism of water loss from the tobacco is assumed to involve a combination of rate-determined and mass-transfer-determined processes.

The evaporation rate of water from a tobacco lamina having a surface area of S and a weight of W at given environmental conditions of temperature, T, and water vapor pressure, P_w, can be expressed [17, 18] by the following empirical equation:

$$\frac{\partial w}{\partial t} = -\left(\frac{S}{W}\right)\alpha \exp\left(-\frac{\theta}{T}\right)(w - w_{eq})^{\beta}. \quad (7)$$

Since the pyrolytic reactions of virgin tobacco at the region where water evaporation is proceeding can be considered to be negligibly slow, Eq. 7 can be used to express the evaporation rate of water from tobacco shreds in the element by replacing the term S/W with N_a/ρ_{vo} as follows:

$$\frac{\partial \rho_w}{\partial t} = \rho_{vo}\frac{\partial w}{\partial t}$$

$$= -N_a\alpha \exp\left(-\frac{\theta}{T}\right)(w - w_{eq})^{\beta}. \quad (8)$$

The equilibrium water content, w_{eq}, of tobacco in Eq. 8 is more directly related to the relative humidity, P_w/P_{ws}, of the environmental gas phase than it is to the temperature [17, 19], as can be seen in the following empirical equation [17]:

$$w_{eq} = \frac{P_w/P_{ws}}{a + b(P_w/P_{ws}) - c(P_w/P_{ws})^2}. \quad (9)$$

The saturated vapor pressure of water, P_{ws}, can be expressed by Calingaert's equation [20] as follows:

$$\log P_{ws} = 7.991 - \frac{1687}{T - 43}. \quad (10)$$

Water-vapor pressure, P_w, inside the element is given by the following mass-balance equation:

$$\frac{\partial}{\partial t}\left(\frac{P_w}{RT}\right) = \frac{\partial}{\partial z}\left\{D_x\frac{\partial}{\partial z}\left(\frac{P_w}{RT}\right)\right\} - \frac{2D_r}{\phi r \delta RT}$$

$$\times\left(P_w - P_{w\infty}\frac{T}{T_\infty}\right) - \frac{\rho_{vo}}{\phi m}\frac{\partial w}{\partial t}. \quad (11)$$

In Eq. 11 the term $\partial(P_w/RT)/\partial t$ represents the net rate of accumulation of water vapor within the element, $\partial[D_x\partial(P_w/RT)/\partial z]/\partial z$ represents the accumulation of water vapor by diffusion through the element, $(2D_r/\phi r\delta RT)(P_w - P_{w\infty}T/T_\infty)$ represents the loss of water vapor by diffusion through a cigarette paper of thickness δ, and $(\rho_{vo}/\phi m)(\partial w/\partial t)$ is the rate of evaporation of water from tobacco.

It has been shown that effective diffusion coefficients of gases such as methane, carbon monoxide, and carbon dioxide through a cigarette column, D_x, and through an ordinary cigarette paper, D_r, are less than the diffusion coefficients, D, in a binary gas mixture by factors of about 2 [10] and 133 [21, 22], respectively. The variation of the binary diffusion coefficient for a water-vapor-air mixture has been presented [23] as follows:

$$D = 0.22\left(\frac{T}{273}\right)^{1.75}. \quad (12)$$

Assuming that the same relations hold for water vapor inside the cigarette column, the effective diffusion coefficients, D_x and D_r, for water vapor can be expressed as follows:

$$D_x = 0.11\left(\frac{T}{273}\right)^{1.75},$$

$$D_r = 1.65 \times 10^{-3}\left(\frac{T}{273}\right)^{1.75}. \quad (13)$$

Heat Balance

The heat balance inside the element can be formulated on the basis of the postulated mechanism, as follows:

$$\frac{\partial}{\partial t}(H_v\rho_v + H_c\rho_c + H_w\rho_w)$$

$$= \frac{\partial}{\partial z}\left(K_e\frac{\partial T}{\partial z}\right) + Q_p\frac{\partial \rho_v}{\partial t} + Q_w\frac{\partial \rho_w}{\partial t}$$

$$-\frac{2}{r}\{h(T - T_\infty) + \sigma\epsilon_s(T^4 - T_\infty{}^4)\}, \quad (14)$$

where H is the specific enthalpy defined as

$$H = \int_{T_\infty}^{T} C_p \, dT = (T - T_\infty) C_p. \tag{15}$$

In Eq. 14 the term $\partial(H_v\rho_v + H_c\rho_c + H_w\rho_w)/\partial t$ represents the net rate of accumulation of heat within the element, $\partial[K_e(\partial T/\partial z)]/\partial z$ represents heat transfer due to thermal conduction, $Q_p(\partial\rho_v/\partial t) + Q_w(\partial\rho_w/\partial t)$ represents the rate of heat loss attributable to pyrolysis and evaporation, and $h(T - T_\infty) + \sigma\epsilon_s(T^4 - T_\infty{}^4)$ is the heat loss by both free convection and radiation from the outer surface of the element.

It has been shown [24] that effective thermal conductivity in highly porous materials can be represented by the following equation:

$$K_e = (1 - \Phi^{2/3})K_s f + \Phi^{1/3}(K_g - \tfrac{2}{3} h_r D_p), \tag{16}$$

where h_r is the heat-transfer coefficient of radiation given by Kunii [24]:

$$h_r = 5.422 \times 10^{-12}\epsilon_t T^3. \tag{17}$$

Since a cigarette column packed with porous tobacco shreds can be considered a type of porous material, Eq. 16 is applicable to the cigarette [12].

The exact value of the free convective heat-transfer coefficient, h, between the outer surface of the cigarette and the surrounding air has not been reported so far as we are aware, although the value of the forced convective heat-transfer coefficient between the tobacco shred and the gas phase inside the cigarette has been published [25]. However, it is well known [26] that the heat-transfer coefficient by free convection from a horizontal pipe to the surrounding air can be represented by the following dimensionless equation:

$$Nu = \frac{2rh}{K_a} = 0.53\,(Gr \cdot Pr)^{0.25}. \tag{18}$$

For air at room temperature and atmospheric pressure, Eq. 18 can be simplified [26] as follows:

$$h = 8 \times 10^{-5}\left(\frac{T - T_\infty}{r}\right)^{0.25}. \tag{19}$$

In the present paper, Eq. 19 is used to estimate the value of h.

Steady-State Equation

The natural smoldering of a cigarette is stationary and proceeds with a constant speed as mentioned above. If the x coordinate, moving at the same speed and in the same direction as the smoldering zone, is taken along the longitudinal axis of the cigarette, the temperature and density profiles will be stationary with respect to the x coordinate. Consequently, Eqs. 5, 6, and 8 can be rewritten as ordinary differential equations (Eqs. 21-23), using the relationships among the x coordinate, the z coordinate, and the smoldering speed expressed by Eq. 20:

$$x = z + ut; \quad \frac{\partial x}{\partial z} = 1; \quad \frac{\partial x}{\partial t} = u, \tag{20}$$

$$\frac{d\rho_v}{dx} = \frac{1}{u}\sum_{i=1}^{4}\left\{-A_i \exp\left(-\frac{E_i}{RT}\right) \times \left(\frac{\rho_{vi}}{\rho_{vi0}}\right)^{n_i}\rho_{vi0}\right\}, \tag{21}$$

$$\frac{d\rho_c}{dx} = -\frac{\rho_f}{\rho_{v0}}\left(\frac{d\rho_v}{dx}\right), \tag{22}$$

$$\frac{d\rho_w}{dx} = \rho_{v0}\frac{dw}{dx} = -\frac{Na}{u}\alpha \exp\left(-\frac{\theta}{T}\right)(w - w_{eq})^\beta. \tag{23}$$

Here, smoldering speed, u, is an imposed parameter and not a part of the solution obtained on integrating the equations.

After some rearrangement Eq. 11 can also be rewritten as

$$\frac{dP_w}{dx} = \frac{-(P_w/T)(d^2T/dx^2) + (2D_r/\phi r\,\delta D_x)[P_w - P_{w\infty}(T/T_\infty)] + (uRT/\phi m D_x)(d\rho_w/dx)}{[(u/D_x) + (2/T)(dT/dx) - (1/D_x)(dD_x/dx)]} + \frac{P_w}{T}\frac{dT}{dx}, \quad (24)$$

where the term dD_x/dx can be derived from Eq. 12 as follows:

$$\frac{dD_x}{dx} = 1.75\,\frac{D_x}{T}\,\frac{dT}{dx}. \quad (25)$$

In Eq. 11 we put the term $\partial^2 P_w/\partial z^2$ as zero, as a first approximation.

Similarly, Eq. 14 can also be rewritten as

$$\frac{dy}{dx} = \frac{1}{K_e}\left\{u(\rho_v C_{pv} + \rho_c C_{pc} + \rho_w C_{pw}) - \frac{dK_e}{dx}\right\} y + \frac{u}{K_e}\left\{(T - T_\infty)\left(C_{pv}\frac{d\rho_v}{dx} + C_{pc}\frac{d\rho_c}{dx} + C_{pw}\frac{d\rho_w}{dx}\right) - Q_p\frac{d\rho_v}{dx} - Q_w\frac{d\rho_w}{dx}\right\} + \frac{2}{rK_e}\{h(T - T_\infty) + \sigma\epsilon_s(T^4 - T_\infty{}^4)\}, \quad (26)$$

where y is defined by

$$\frac{dT}{dx} = y. \quad (27)$$

Assuming that all parameters in Eq. 16 except h_r are constant throughout the evaporation-pyrolysis process, the term dK_e/dx in Eq. 26 can be given as

$$\frac{dK_e}{dx} = 2D_p\Phi^{1/3}\,\frac{h_r}{T}\,\frac{dT}{dx}. \quad (28)$$

NUMERICAL SOLUTION

The set of simultaneous first-order ordinary differential equations made up of Eqs. 21-24, 26, and 27 can be solved numerically using the Runge-Kutta-Gill method [27] assuming given initial conditions, reasonable physical parameters and a step size of 0.025 mm.

Initial Conditions

The initial value for y, or dT/dx, can be calculated as follows. If the temperature is low enough, the pyrolysis of virgin tobacco, the evaporation of water, and the heat transfer due to free convection and radiation can be ignored; Eq. 26 then becomes:

$$\frac{d^2T}{dx^2} = \frac{u}{K_e}(\rho_{v0}C_{pv} + \rho_{w0}C_{pw})\frac{dT}{dx}. \quad (29)$$

Solving Eq. 29 with the use of boundary conditions, $T = T_\infty$ at $x = -\infty$ and $T = T_0$ at $x = x_0$, yields

$$T = (T_0 - T_\infty)\exp\left\{\frac{u}{K_e}(\rho_{v0}C_{pv} + \rho_{w0}C_{pw})(x - x_0)\right\} + T_\infty. \quad (30)$$

Accordingly, the initial value for y corresponding to x_0 and T_0 is given by

$$y_0 = \left(\frac{dT}{dx}\right)_0 = \frac{u}{K_e}(T_0 - T_\infty)(\rho_{v0}C_{pv} + \rho_{w0}C_{pw}). \quad (31)$$

The value for x_0 was chosen to be $x_0 = 0$. The choice of the value for T_0 involves a slight problem because the solutions are somewhat sensitive to T_0, particularly for relatively high T_0 values. This indicates that Eqs. 29-31 are set up only when the local temperature inside a cigarette is in the vicinity of the ambient air temperature, T_∞(293 K). Consequently, a value for T_0 of 294 K has been used.

Suppose the local mole concentration of water vapor in a low-temperature region in the vicinity of T_∞ is equal to that in ambient air with a relative humidity of 60%. Then the initial value for water-vapor pressure, P_w, is given by

$$P_{w0} = P_{w\infty} \frac{T_0}{T_\infty} = 10.53 \text{ (mm Hg)}.$$

The values for ρ_{a0}, ρ_{w0}, and ρ_{v0} are given by

$$\rho_{a0} = \frac{\text{cigarette weight}}{\text{cigarette volume}} \text{ (g/cm}^3\text{)},$$

$$\rho_{w0} = \rho_{a0} \frac{\omega_0}{1 + \omega_0},$$

$$\rho_{v0} = \rho_{a0} - \rho_{w0},$$

and needless to say,

$$\rho_{c0} = 0.$$

The values for ρ_{a0} and w_0 are shown in the fifth and sixth columns of Table 1, respectively.

Physical Parameters

The values of the physical parameters used to solve the simultaneous differential equations are summarized in Table 2. Some were experimentally measured as a part of this work; others were obtained from the literature.

Apparent kinetic parameters for tobacco pyrolysis have been published recently [28-31]; however, there are insufficient kinetic data to account for the weight loss attributable to pyrolysis. The apparent kinetic parameters shown in Table 2(a) were derived from the analysis of thermogravimetric-derivative thermogravimetric (TG-DTG) curves of tobacco obtained in a helium atmosphere over a wide range of heating rates (2.5-240°C/min), with the aid of a rapid-heating thermobalance equipped with an infrared (IR) image furnace [31]. The TG-DTG curves showed that the complex pyrolytic reactions of tobacco consist of four major steps. Assuming that each step corresponds to the pyrolysis of major compounds in tobacco, four sets of apparent kinetic parameters were determined as outlined in an earlier paper [31].

The values for experimental constants related to water loss, that is, a, b, c, α, β, and θ, were obtained from Samejima's data [18]. The value for void fraction, ϕ, inside a cigarette (here, the pores of tobacco shred are not regarded as void space) was determined as follows:

$$\phi = 1 - \frac{\text{packing density of shred}}{\text{apparent density of shred}}.$$

The value for total void fraction, Φ, inside a cigarette (here, the pores of tobacco shred are regarded as void space) was calculated using:

$$\Phi = 1 - \frac{\text{packing density of shred}}{\text{real density of shred}}.$$

Apparent and real density values of shred are shown in the seventh and eighth columns of Table 1, respectively.

An average tobacco shred is about 5 mm long and 0.65 mm wide, but its thickness depends on the tobacco type, that is 0.12 mm for flue-cured, 0.08 mm for Burley, and 0.09 mm for Matsukawa [32]. Therefore, the surface area of one shred of flue-cured tobacco is 0.07856 cm^2, and its volume is 3.9×10^{-4} cm^3. Consequently, the average number and the total surface area, N_a, of tobacco shred per cubic centimeter inside a flue-cured cigarette with a packing fraction, $1 - \phi$, of 0.341 are 874 and 68.7 cm^2, respectively, as shown in Table 2(b).

If the radiating area inside a cigarette is assumed to be equal to the total surface area of the shred and the void space is regarded as a gathering of spherical pores, the value for apparent average diameter, D_p, of the pore can be estimated from the following equation:

$$D_p = \frac{6\phi}{N_a}.$$

The effective thermal conductivity [12, 33] of tobacco shred depends on tobacco type, packing density, temperature, and other parameters. However, our experimental results [12] have shown

TABLE 2

Physical Parameters Used for Calculations[a]

	Flue Cured	Burley	Matsukawa			
	(F)	(B)	(M_1)	(M_2)	(M_3)	Reference
	(a) Apparent Kinetic Parameters of Pyrolytic Reactions					
$i = 1$						
n	1	1	1	1	1	
E (kcal/mole)	20.2	20.8	20.8	20.8	20.8	
A (1/sec)	6.27×10^7	1.00×10^8	1.00×10^8	1.00×10^8	1.00×10^8	
Contribution to pyrolysis	0.25	0.08	0.05	0.05	0.05	
$i = 2$						
n	1	1	1	1	1	
E	24.5	25.6	20.1	20.1	20.1	
A	1.69×10^8	7.31×10^8	4.08×10^6	4.08×10^6	4.08×10^6	
Contribution to pyrolysis	0.28	0.32	0.35	0.35	0.35	
$i = 3$						
n	1	1	1	1	1	
E	45.7	39.8	40.2	40.2	40.2	
A	5.99×10^{14}	1.32×10^{13}	8.65×10^{12}	8.65×10^{12}	8.65×10^{12}	
Contribution to pyrolysis	0.17	0.30	0.30	0.30	0.30	
$i = 4$						
n	3	3	3	3	3	
E	25.2	27.9	29.1	29.1	29.1	
A	4.69×10^6	2.64×10^7	6.12×10^7	6.12×10^7	6.12×10^7	
Contribution to pyrolysis	0.30	0.30	0.30	0.30	0.30	
	(b) Paremeters Related to Water Loss					
a	5.12	1.76	1.76	1.76	1.76	18
b	8.46	17.38	17.38	17.38	17.38	18
c	14.16	17.92	17.92	17.92	17.92	18
α (g/sec·cm^2)	1.345×10^7	1.345×10^7	1.345×10^7	1.345×10^7	1.345×10^7	18
β	1.81	1.81	1.81	1.81	1.81	18
θ (K)	8430	8430	8430	8430	8430	18
N_a (cm^2/cm^3)	68.7	99.0	78.1	88.8	108.9	
ϕ	0.659	0.652	0.691	0.654	0.576	
$P_{w\infty}$ (mm Hg)	10.50	10.50	10.50	10.50	10.50	
	(c) Parameters Related to Heat Balance					
C_{pv} (cal/g·K)	0.41	0.34	0.35	0.35	0.35	12
C_{pc} (cal/g·K)	0.25	0.25	0.25	0.25	0.25	12
C_{pw} (cal/g·K)	1.00	1.00	1.00	1.00	1.00	12
$K_s f$ (cal/sec·cm·K)	7.56×10^{-4}	7.56×10^{-4}	7.56×10^{-4}	7.56×10^{-4}	7.56×10^{-4}	12
K_g (cal/sec·cm·K)	1.08×10^{-4}	1.08×10^{-4}	1.08×10^{-4}	1.08×10^{-4}	1.08×10^{-4}	12
ϵ_s, ϵ_t	0.97	0.97	0.97	0.97	0.97	39
D_p (cm)	0.0575	0.0395	0.0535	0.0442	0.0317	
Φ	0.798	0.822	0.849	0.828	0.789	
Q_w (cal/g)	540	540	540	540	540	
Q_p (cal/g)	0	0	0	0	0	

TABLE 2 (Continued)

Physical Parameters Used for Calculations[a]

	Flue Cured	Burley	Matsukawa			
	(F)	(B)	(M_1)	(M_2)	(M_3)	Reference
			(d) Other Parameters			
u (cm/min)	4.43×10^{-3}	6.33×10^{-3}	6.31×10^{-3}	5.38×10^{-3}	4.78×10^{-3}	
δ (cm)	3.70×10^{-3}	3.70×10^{-3}	3.70×10^{-3}	3.70×10^{-3}	3.70×10^{-3}	
T_∞ (K)	293	293	293	293	293	

[a] See Nomenclature section.

that the effective thermal conductivity of conditioned shred can be uniformly expressed by Kunii's equation (Eq. 16) as a function of the total void fraction regardless of tobacco type. This work also gave the values for the apparent thermal conductivity of solid and gas phases inside the cigarette as listed in Table 2(c). Calculated effective thermal conductivity values for cigarettes used in this paper are in the range of $1.85\text{-}2.13 \times 10^{-4}$ cal/sec·cm·K at 20°C. These values are the same order of magnitude as those reported by Samfield and Brock [33].

The specific heat [12, 34, 35] of virgin tobacco, C_{pv}, depends on tobacco type and temperature. A mean value [12] over the temperature range 323-373 K has been used in calculations, as well as the value for char, C_{pc}.

Tiller et al. [28] and Edmonds et al. [36] have observed endothermic peaks on DTA curves attributable to pyrolytic reactions, when tobacco is heated in an inert atmosphere. Reliable knowledge about the value of heat of pyrolytic reactions, Q_p, of tobacco, however, is lacking as far as we are aware. Thermal analysis of tobacco and its constituents in a helium atmosphere with the aid of a differential scanning calorimeter (DSC) suggests [37] that the pyrolysis of α-cellulose in tobacco is a typical endothermic reaction, whereas the pyrolysis of some constituents (e.g., pectin) is exothermic in the presence of some inorganic impurities. Accordingly, since exothermic and endothermic reactions tend to compensate for each other, endothermic peaks observed on DSC curves of tobacco pyrolysis [37] are very small and indistinct compared with the peak for α-cellulose. For reference, according to the report by Tang and Neill [38], the heat of pyrolysis of α-cellulose is 88 cal/g. For this reason, heat of pyrolysis of tobacco was ignored in the present paper.

All parameters mentioned in this section or listed in Table 2 were regarded as being constant throughout the evaporation-pyrolysis process.

THEORETICAL RESULTS AND DISCUSSIONS

Figure 6 shows typical profiles of temperature, density, and water vapor pressure calculated for a cigarette containing flue-cured tobacco. A visible decrease in density owing to evaporation begins at near 60°C. A rapid decrease in density owing to pyrolysis follows in the temperature range of about 200-400°C. Finally, a gradual decrease occurs at higher temperatures. These curves calculated from our theoretical model are in agreement with experimental data presented earlier. Figure 6 indicates that the evaporation of water from tobacco takes place in the region of 60-200°C prior to pyrolysis of virgin tobacco. Thus, on the basis of postulated mechanisms of smoldering, the evaporation region is clearly distinguishable from the pyrolysis region.

A theoretical profile of the water-vapor pressure in the gas phase is also shown in Fig. 6. However, we cannot evaluate its validity since a profile of the water-vapor pressure inside a smoldering cigarette has not been determined experimentally.

Theoretical profiles of temperature and density are shown in Fig. 7 for cigarettes of different

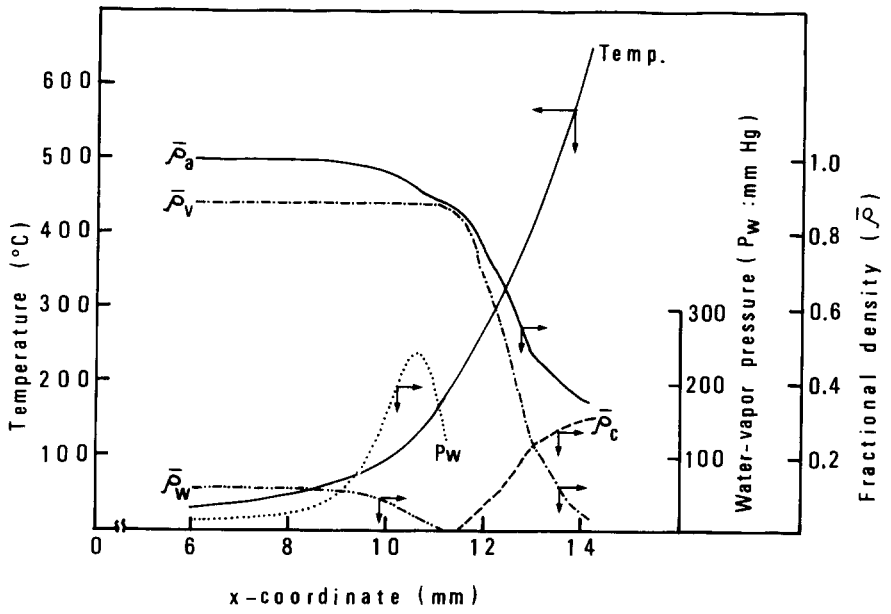

Fig. 6. Theoretical profiles of temperature, density, and water-vapor pressure in evaporation-pyrolysis zone of a cigarette containing flue-cured tobacco.

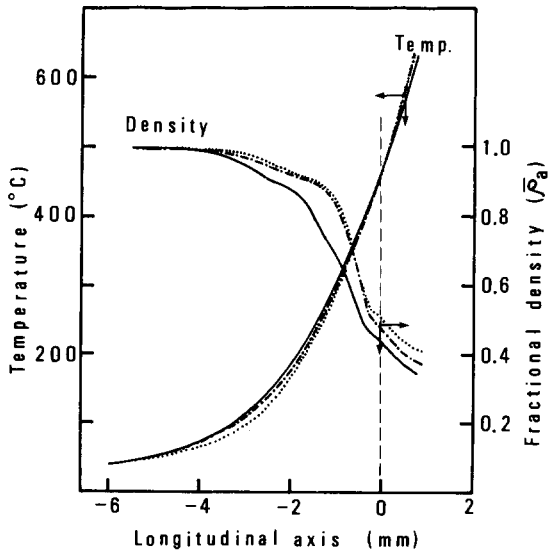

Fig. 7. Comparison of theoretical temperature and density profiles for cigarettes containing different types of tobacco: — , flue cured (F); · · · ·, burley (B); -·-·-·-, Matsukawa (M_2).

tobacco types. The position of the paper char line, of course, is not obtained by integrating the equations. Rather, the char line is assumed to correspond to the point where the temperature is 450°C. The char line has been assigned the axial position of zero in all of the profiles except Fig. 6.

As can be seen in Fig. 7, the theoretical analysis predicts that there is no significant difference in the temperature profiles among the cigarettes; the experimental results mentioned above support this finding. On the other hand, the theoretical density profiles differ slightly. This difference in density depends primarily on the kinetic parameters used in the calculations. Actually, the original TG curves from which the kinetic parameters were determined differed among the tobacco types [37]. There was little difference in theoretical temperature and density profiles among cigarettes of different packing density (these data have not been presented).

Figure 8 compares calculated temperature and density profiles with experimental ones. The calculated temperature profile almost agrees with the experimental profile, and the density profile ap-

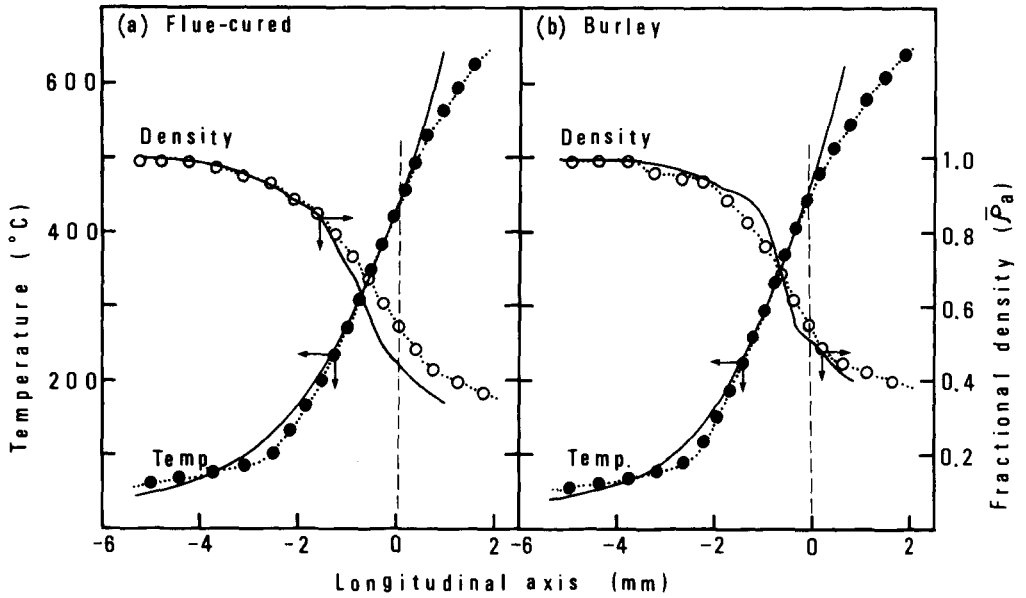

Fig. 8. Comparison of theoretical and experimental temperature and density profiles in evaporation-pyrolysis zone: ——, theoretical; ··o···o·· and ··●···●··, experimental.

proximately agrees with the experimental profile. The slight discrepancy observed in Fig. 8 between the theoretical and experimental profiles, although not sufficiently significant to reduce the reliability of the proposed model, may arise from unavoidable experimental errors accompanying the measurement of the density profile or other measured physical parameters as well as from simplification of the model. For example, the slit diameter of the collimator used to measure the density profiles may be rather large (1 mm) compared with the thickness of the evaporation-pyrolysis zone indicated in Fig. 2.

The agreement between theoretical and experimental results suggests that the proposed model should be able to account for the fundamental evaporation-pyrolysis processes occurring in the naturally smoldering cigarette. Moreover, the model can be used to evaluate the relative magnitudes of the many parameters that govern the shapes of the temperature and density profiles.

Figures 9 and 10 illustrate the influence of smoldering speed and thermal conductivity of the tobacco solid, respectively, on the shapes of the temperature and density profiles. Specific values used for the calculations are given in the figure legends. Other parameters are the same as those for cigarettes containing flue-cured tobacco listed in Table 2.

Each of these parameters evidently affects the temperature and density profiles and the thickness of the evaporation-pyrolysis zone. An increase in smoldering speed (Fig. 9) results in an increase in the gradient of the temperature profile and a decrease in the thickness of the evaporation-pyrolysis zone. A similar tendency was observed for packing density, specific heat, free convective heat-transfer coefficient, radiative emissivity at the outer surface of the cigarette, and water content in the tobacco. On the other hand, an increase in effective thermal-conductivity value results in a decrease in the temperature gradient and an increase in the thickness of the evaporation-pyrolysis zone as shown in Fig. 10.

The variation in the density profiles observed in Figs. 9 and 10 results largely from the variation

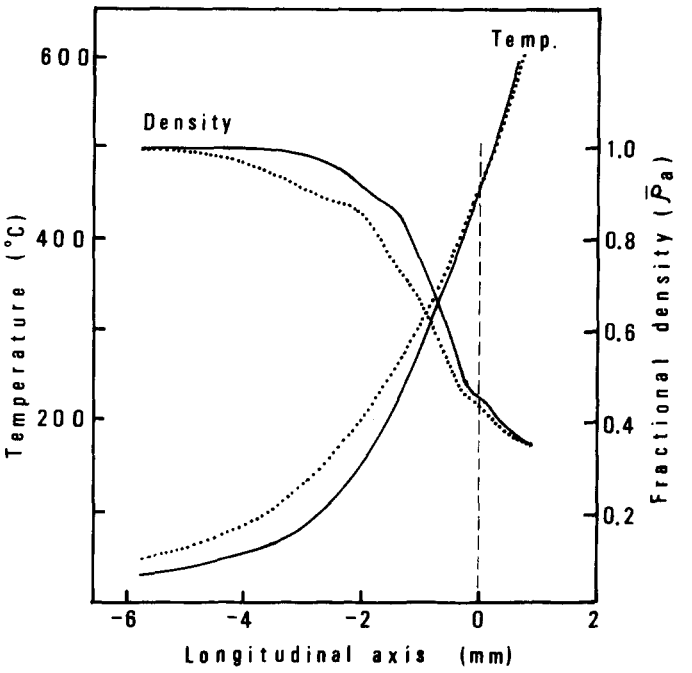

Fig. 9. Influence of smoldering speed on shapes of theoretical temperature and density profiles for cigarettes containing flue-cured tobacco: ·····, $u = 3.0 \times 10^{-3}$ cm/sec; ——, $u = 6.67 \times 10^{-3}$ cm/sec.

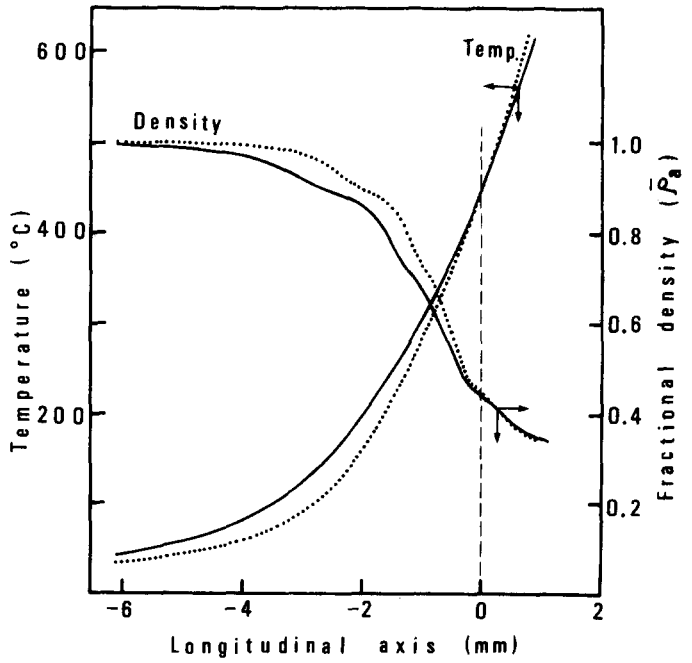

Fig. 10. Influence of thermal conductivity of tobacco solid on shapes of theoretical temperature and density profiles for cigarettes containing flue-cured tobacco: ·····, $K_s f = 5.04 \times 10^{-4}$ cal/sec·cm·K; ——, $K_s f = 11.34 \times 10^{-4}$ cal/sec·cm·K.

in the temperature profiles, becuase the density profile depends on temperature as well as kinetic parameters.

The authors wish to thank Dr. Yoshida for his advice on the measurement of β-ray absorption and Mr. Samejima for providing the data related to water loss from tobacco.

NOMENCLATURE

A	preexponential factor (1/sec)
C	conversion (–)
C_p	specific heat (cal/g•k)
D	binary diffusion coefficient of water vapor in air (cm^2/sec)
D_r	effective diffusion coefficient of water vapor through a cigarette paper (cm^2/sec)
D_x	effective diffusion coefficient of water vapor inside a cigarette column (cm^2/sec)
D_p	average diameter of void space inside a cigarette (cm)
E	activation energy (cal/mole)
Gr	Grashoff number (–)
H	specific enthalpy (cal/g)
I	counting rate of β-rays after passage through an absorbing material (cpm)
I_0	counting rate of β-rays without absorbing material (cpm)
K_e	effective thermal conductivity of a cigarette (cal/sec•cm•K)
K_g	thermal conductivity of the gas phase inside a cigarette (cal/sec•cm•K)
K_s	thermal conductivity of tobacco solid (cal/sec•cm•K)
N_a	total surface area of tobacco shreds per unit volume of a cigarette (cm^2/cm^3)
Nu	Nusselt number (–)
Pr	Prandtl number (–)
P_w	water-vapor pressure inside a cigarette or environmental air (mm Hg)
P_{ws}	saturated water vapor (mm Hg)
Q_p	heat of pyrolysis (cal/g)
Q_w	heat of evaporation (cal/g)
R	gas constant (1.98 cal/mole•K or 6.23 × 10^4 cm^3•mm Hg/mole•K)
S	surface area of a tobacco lamina (cm^2)
T	temperature (K)
W	weight of a tobacco lamina (g)
a, b, c	experimental constants (–)
f	correction factor (–)
h	free convective heat-transfer coefficient (cal/sec•cm^2•K)
h_r	heat-transfer coefficient of radiation (cal/sec•cm^2•K)
i	tobacco component number ($i = 1, 2, 3, 4$)
m	mass number of water (18.0 g/mole)
n	order of pyrolitic reaction (–)
r	radius of cigarette (cm)
t	time (sec)
u	smoldering speed (cm/sec)
w	water content in tobacco (g H_2O/g tobacco)
w_{eq}	equilibrium water content in tobacco (g H_2O/g tobacco)
α	experimental constant (g/sec•cm^2)
β	experimental constant (–)
δ	thickness of a cigarette paper (cm)
σ	Stefan-Boltzmann constant (1.355 × 10^{-12} cal/sec•cm^2•K^4)
ϕ	void fraction inside a cigarette based on apparent density (–)
Φ	total void fraction inside a cigarette based on real density (–)
θ	experimental constant (K)
ρ	density (g/cm^3)
$\bar{\rho}$	fractional density given by ρ/ρ_{a0} (–)
ϵ_s	radiative emissivity of outer surface of a cigarette (–)
ϵ_t	radiative emissivity of tobacco shred inside a cigarette (–)

Subscripts

a	total value, (i.e., ρ_a represents total density)
c	char
f	final value (i.e., ρ_f represents density of char remaining after completion of pyrolysis)
0	initial value
v	virgin tobacco
w	water
∞	environmental air condition

REFERENCES

1. Baker, R. R., and Kilburn, K. D., *Beitr. Tabakforsch.* 7:79 (1973).
2. Touey, G. P., and Mumpower, R. C., II, *Tobacco Sci.* 1:33 (1957).
3. Adams, P. I., *Tobacco Sci.* 12:144 (1968).
4. Muramatsu, M., Obi, Y., Fukuzumi, T., and Keii, T., *J. Agric. Chem. Soc. Jap.* 46:569 (1972), *Heat Transf.-Jap. Res. (USA)* 2(2):7 (1973).
5. Baker, R. R., *Nature* 247:405 (1974).
6. Baker, R. R., *High Temp. Sci.* 7:236 (1975).
7. Egerton, A., Gugan, K., and Weinberg, F. J., *Combust. Flame* 7:63 (1963).
8. Gugan, K., *Combust. Flame* 10:161 (1966).
9. Jenkins, R. W., Frisch, A. F., Mackinnon, J. G., and Williamson, T. G., *Beitr. Tabakforsch.* 9:67 (1977).
10. Baker, R. R., *Combust. Flame* 30:21 (1977).
11. Moussa, N. A., Toong, T. Y., and Darris, C. A., *Sixteenth Symposium (International) on Combustion,* The Combustion Institute, Pittsburgh, 1977, p. 1447.
12. Muramatsu, M., Umemura, S., and Okada, T. (in press).
13. Muramatsu, M., Umemura, S., and Okada, T., *J. Chem. Soc. Jap. Chem. Ind. Chem.* 1441 (1978).
14. Savitzky, A., and Golay, M. J. E., *Anal. Chem.* 36: 1627 (1964).
15. Comar, C. L., *Radioisotopes in Biology and Agriculture,* McGraw-Hill, New York, 1955, p. 86.
16. Baker, R. R., *Anal. Calorim.* 4:193 (1977).
17. Kamei, S., and Suzuki, S., *J. Soc. Chem. Ind. Jap.* 44:351 (1941).
18. Samejima, T., unpublished results.
19. Masuo, Y., Tsuzuki, K., and Katayama, Y., *Sci. Paper, Cent. Res. Inst., Jap. Monop. Corp.* (106):27 (1964).
20. Calingaert, G., and Davis, D. S., *Ind. Eng. Chem.* 17: 1287 (1925).
21. Owen, W. C., and Reynolds, M. L., *Tobacco Sci.* 11:14 (1967).
22. Muramatsu, M., Mikami, Y., Naitō, N., and Tomita, H., *Beitr. Tabakforsch.* 9:141 (1977).
23. *International Critical Tables* (E. W. Washburn, Ed.), McGraw-Hill, New York, 1929, Vol. 5, p. 62.
24. Kunii, D., *Chem. Eng. (Jap.)* 25:891 (1961).
25. Sandusky, T., Ohlemiller, T. J., and Summerfield, M., *Beitr. Tabakforsch.* 9:117 (1977).
26. McAdams, W. H., *Heat Transmission,* 2nd Ed., McGraw-Hill, New York, 1942, p. 237.
27. Amemiya, A., and Taguchi, T., *Suchikaiseki to FORTRAN,* Maruzen, Tokyo, 1969, p. 358.
28. Tiller, C. O., and Gentry, E. M., *Beitr. Tabakforsch.* 9:7 (1977).
29. Baker, R. R., *Thermochim. Acta* 17:29 (1976).
30. Baker, R. R., *Thermochim. Acta* 23:201 (1978).
31. Muramatsu, M., *Netsu Sokutei* 5:82 (1978).
32. Okada, T., and Ōta, K., *Sci. Paper, Cent. Res. Inst., Jap. Tobacco & Salt Pub. Corp.* (117):11 (1975).
33. Samfield, M., and Brock, B. A., *Tobacco Sci.* 2:49 (1958).
34. Brock, B. A., and Samfield, M., *Tobacco Sci.* 2:41, 45 (1958).
35. Chakrabariti, S. M., and Johnson, W. H., *Transact. ASAE* 15:928 (1972).
36. Edomods, M. D., Core, M. T., and Bavley, A., *Tobacco Sci.* 9:48 (1965).
37. Muramatsu, M., and S. Umemura, unpublished results.
38. Tang, W. K., and Neill, W. K., *J. Polym. Sci., Part C* 6:65 (1964).
39. Lendvay, A. T., and Laszlo, T. S., *Beitr. Tabakforsch.* 8:283 (1976).

Received 16 October 1978; revised 20 April 1979